

Sevoflurane inhibits the malignant behavior of nasopharyngeal carcinoma cells by regulating mitochondrial membrane potential

Xuan Peng¹ and YuLin Zhou²

¹ Department of Anesthesia Surgery, The First People's Hospital of Shuangliu District, Chengdu City, Sichuan Province, China

² Department of Otorhinolaryngology-Head and Neck Surgery, The First Affiliated Hospital of Chengdu Medical College, Chengdu City, Sichuan Province, China

Abstract. This study aims to determine the effect of sevoflurane (Sev) on nasopharyngeal carcinoma (NPC) in malignant behavior and mitochondrial membrane potential (MMP). NPC cells (5-8F and CNE2) were exposed to Sev at different concentrations and then tested for proliferation by CCK-8 and colony formation assays, apoptosis by flow cytometry, and invasion and migration by Transwell assays. In addition, the Warburg effect was examined by measurements of glucose consumption, lactic acid production, and adenosine triphosphate (ATP). Mitochondrial function was evaluated by reactive oxygen species (ROS) production, oxidative stress-related indexes, and mitochondrial membrane potential. Sev suppressed 5-8F and CNE2 cell proliferation, invasion, and migration, and enhanced apoptosis. Moreover, Sev dampened the Warburg effect by reducing glucose consumption, lactic acid production, and ATP, as well as decreasing hexokinase 2 and pyruvate kinases type M2 protein expressions. Also, Sev induced ROS production and malondialdehyde content and reduced superoxide and glutathione peroxidase levels. Finally, Sev caused damage to mitochondrial homeostasis through induction of cleaved caspase-3, cleaved caspase-9, and cytochrome c protein expression and reduction of MMP. Sev inhibits the malignant behavior of NPC cells by regulating MMP.

Key words: Sevoflurane — Nasopharyngeal carcinoma — Mitochondrial membrane potential — ROS production — Warburg effect

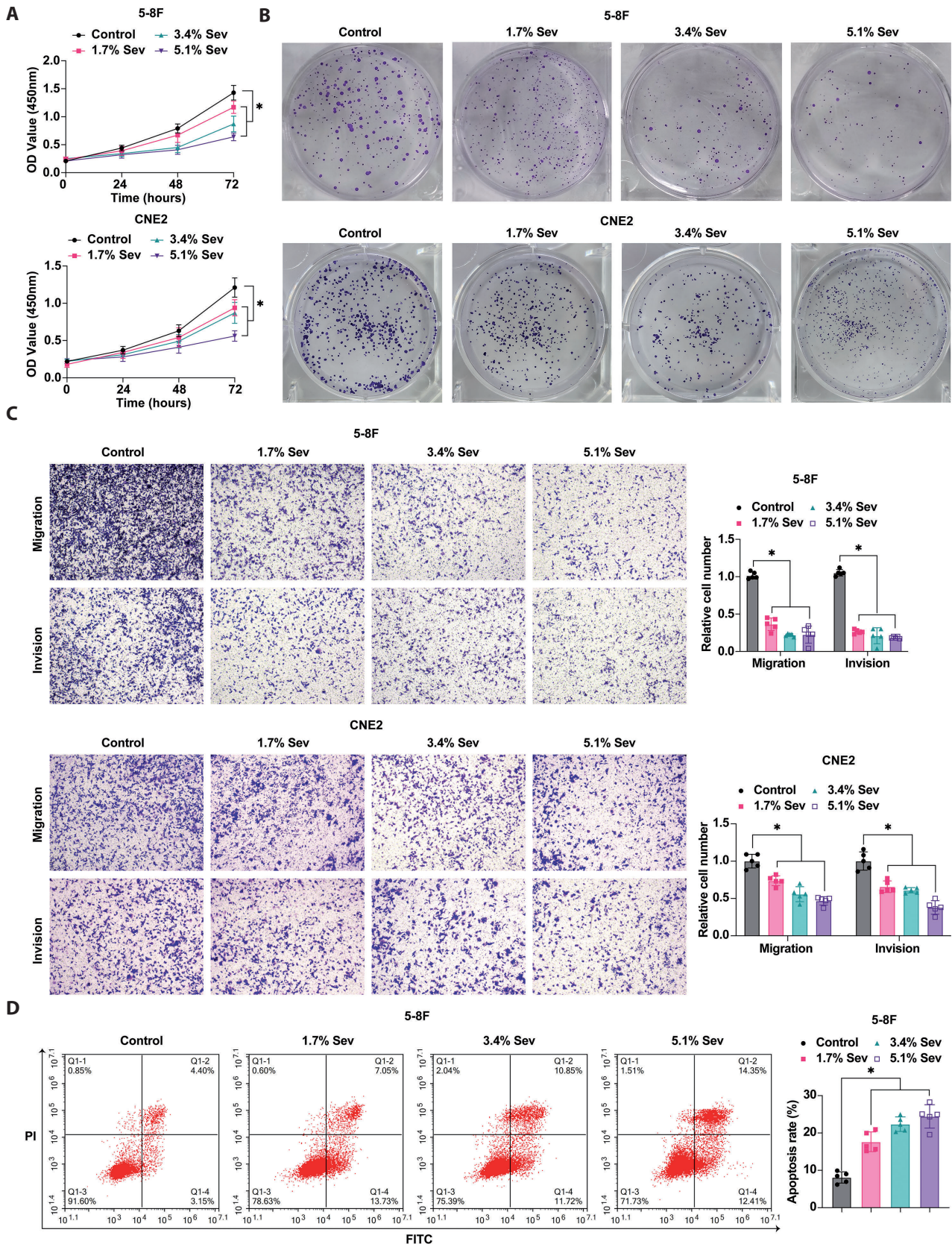
Introduction

The term “nasopharyngeal carcinoma (NPC)” refers to all squamous cell carcinomas including keratinized, non-keratinized, and basaloid carcinoma subtypes (Bossi et al. 2021). NPC is a malignant epithelial tumor occurring in the mucosa of the nasopharynx, and its endemic variation is always associated with Epstein-Barr virus and usually manifests as undifferentiated histological subtypes (Chua et al. 2019). It is thought that differences in dietary habits, lifestyle, and exposure to harmful environmental factors

may be the root cause of the geographical differences in the incidence of NPC (Lee et al. 2019). At present, in addition to minimally invasive surgery and immunotherapy, intensity-modulated radiotherapy and chemotherapy strategies have contributed to improved survival and reduced toxicity (Lam and Chan 2018; Chen et al. 2019).

It is well-known that mitochondrial dysfunction is a hallmark of tumors, and targeting tumor mitochondria has become a promising anticancer therapy. In particular, unique mitochondrial characteristics in tumors have been used as targets, signals, triggers, or driving forces for specific sensing/diagnostic/imaging of characteristic mitochondrial changes, delivery of targeted drugs on mitochondria, delivery/accumulation of targeted drugs on mitochondria, or stimulus-induced drug release in mitochondria (Cho et al. 2020). In tumor tissues, mitochondria can alter metabolic phenotypes to meet high energy requirements and the challenges of macromo-

Correspondence to: YuLin Zhou, Department of Otorhinolaryngology-Head and Neck Surgery, The First Affiliated Hospital of Chengdu Medical College, No. 278 Baoguang Avenue, Xindu District, Chengdu City, Sichuan Province, 610500, China
E-mail: zyl4711@hotmail.com



(continued)

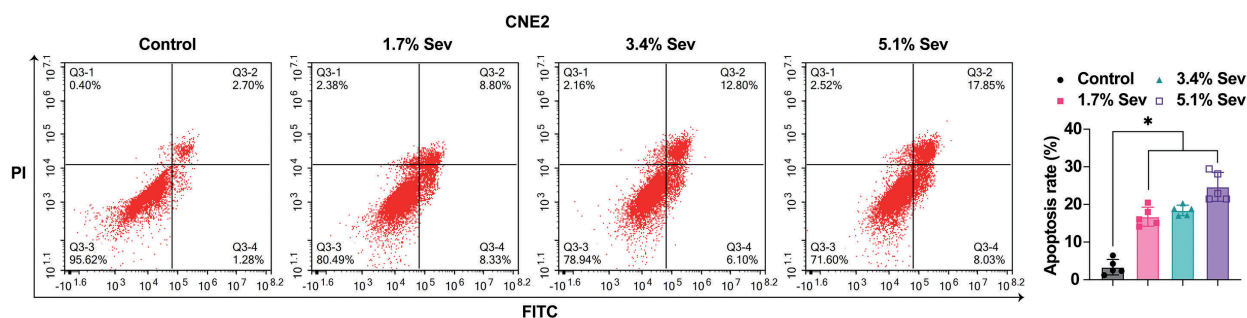


Figure 1. Sev inhibits the malignant behaviors of NPC cells. Cell proliferation rate was detected by CCK-8 assay (A) and colony formation assay (B). C. Cell invasion and migration were assessed by Transwell assays. D. Cell apoptosis rate was calculated by flow cytometry. Data were expressed as mean \pm SD ($n = 5$). * $p < 0.05$. NPC, nasopharyngeal carcinoma; Sev, sevoflurane.

lecular synthesis. In addition, mitochondria can crosstalk the tumor microenvironment, and signals from cancer-associated fibroblasts can shock mitochondria (Roth et al. 2020). Sevoflurane (Sev) was first discovered by Ross Terrell, synthesized by Regan in 1968, completed phase III clinical trials in 1986, and was first approved for clinical use by the Japanese drug administration in 1990. The LD50 of Sev in rats is 0.47 ml/kg (Morohashi et al. 2016). In recent years, it has been praised as a landmark drug in inhalation anesthesia by many famous anesthesiologists (Terrell 2008). Sev has been shown to inhibit the development and progression of tumors through a variety of pathways. For example, high concentrations of Sev (4%) increase the rate of apoptosis of breast cancer cells by regulating calcium homeostasis (Deng et al. 2020). Sev can also inhibit the proliferation and migration of gastric cancer cells (Yong et al. 2021). Notably, Sev has been found to modulate mitochondrial dysfunction to influence nerve cell iron death as well as neuronal damage (Zhang et al. 2020; Zhang et al. 2022). In cancer cells, Sev can inhibit the proliferation and invasion by interfering with mitochondrial function of cells, which is mainly achieved by activating the Ca^{2+} dependent calmodulin-dependent protein kinase II/c-Jun N-terminal kinase cascade (Han et al. 2020). However, the effect of Sev on mitochondrial function in NPC cell lines remains unclear.

Considering the significance of mitochondrial function, the current study exploited whether Sev interferes with tumor progression in NPC by modifying mitochondrial membrane potential (MMP), targeting to support the clinical application of Sev in tumor therapy.

Materials and Methods

Cell culture

NPC cells 5-8F (C486) and CNE2 (C488) (Shanghai Enzyme-linked Biotechnology Co., Ltd., China) were cultured in RPMI-1640 medium (Gibco) containing 10% fetal bovine

serum (Gibco) and kept in a humid incubator at 37°C and 5% CO_2 . The cells were identified by STR (short tandem repeat).

Sev exposure

5-8F and CNE2 cells were placed in an airtight container in a humid environment of 37°C. Sev (Seebio Biotech, Shanghai) was mixed with 95% air and 5% CO_2 in a volatile tank and its concentration was adjusted to 1.7%, 3.4%, and 5.1%, respectively using a gas monitor (PM 8060; Dräger). 5-8F and CNE2 cells were then treated with different concentrations of Sev for 6 h. Normal air-treated 5-8F and CNE2 cells served as a control group.

Cell counting kit (CCK)-8 experiment

5-8F cells and CNE2 were inoculated into 96-well plates at 5000 cells/well, with 5 repeat wells set for each sample. Next, 100 μ l culture medium was introduced into each well, and 10 μ l CCK-8 solution (Dojindo, Japan) was given at different time points (24, 48, and 72 h) and incubated without light exposure for another 2 h. Absorbance was measured at 450 nm using a microplate reader (Thermo Fisher, USA).

Colony formation experiment

5-8F and CNE2 cells (about 4×10^3 cells/wells) were inoculated in 6-well plates overnight, treated with Sev, and then allowed to grow for 14 days, changing the medium every 3 days. On day 14, cells were fixed with 4% paraformaldehyde for 15 min and then stained with crystal violet dye for 25 min. Then, each well was rinsed with phosphate buffered saline (PBS) and then allowed to air dry. The colonies were then counted using ImageJ software.

Apoptosis analysis

5-8F and CNE2 cells were analyzed with Annexin V-Fluorescein isothiocyanate (FITC) apoptosis detection kit (Vazyme).

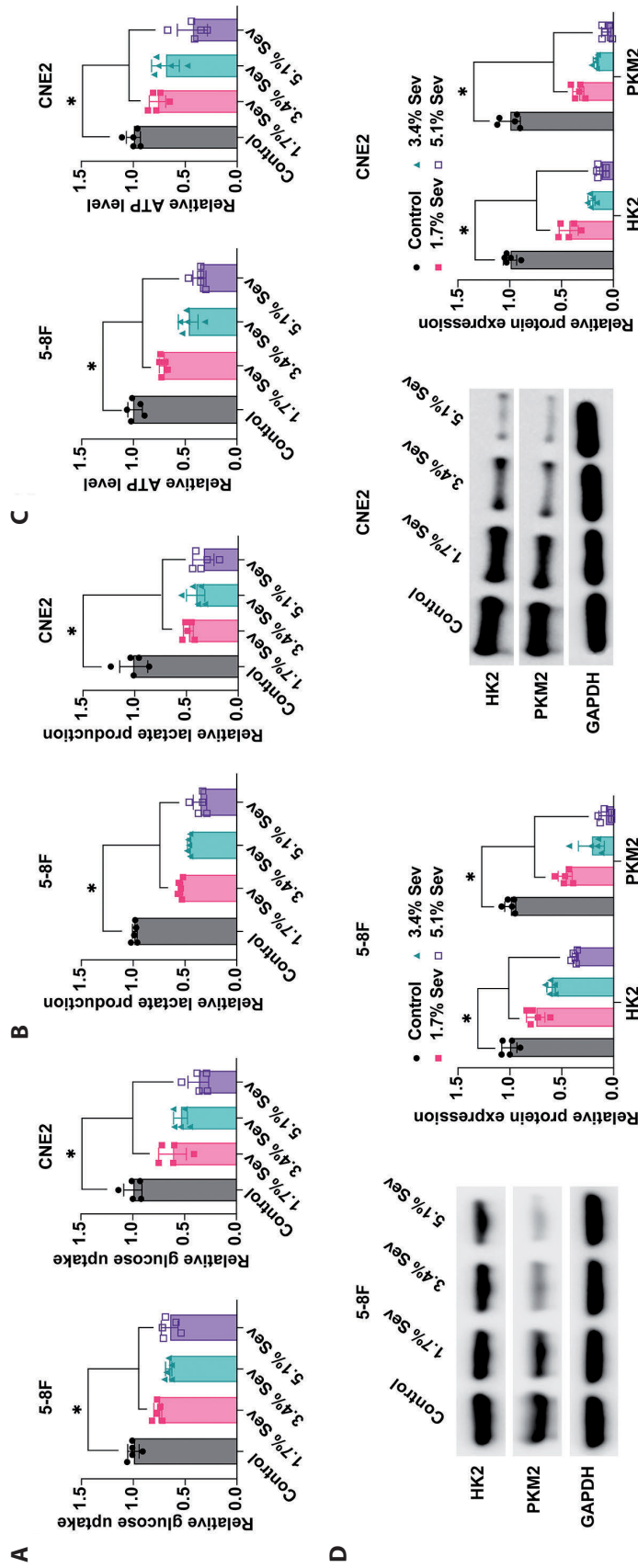


Figure 2. Sev effectively reduces Warburg effect of NPC. Commercial kits detected cellular glucose consumption (A), lactic acid production (B), and ATP level (C). D. Hexokinase 2 (HK2) and pyruvate kinases type M2 (PKM2) were detected by Western blot assay. Data were expressed as mean \pm SD ($n = 5$). * $p < 0.05$. For more abbreviations, see Figure 1.

Cells were rinsed with cold PBS (Sangon, Shanghai, China) and resuspended in a binding buffer, followed by a mixture with 5 μ l Annexin V-FITC and 5 μ l propidium iodide and culture darkly at room temperature for 15 min. Finally, apoptosis was estimated by flow cytometry (Beckman Coulter, USA).

Transwell assays

Transwell chambers (Corning, USA) with an 8 μ m pore size polycarbonate filter were utilized to assess migration and invasion of 5-8F and CNE2 cells. 5×10^4 cells from serum-free medium were inoculated into the upper cavity pre-covered or uncovered with Matrigel (Corning, BD356230). In the meantime, 600 μ l 10% fetal bovine serum medium was added to the lower cavity. After culture, the cells were removed from the upper surface of the filter. Cells that migrated or invaded the lower surface of the filter were then immobilized in 95% ethanol for 15 min and stained with 0.1% crystal violet for 20 min, which were measured and averaged under a microscope (Leica Microsystems, Germany) in 5 regions.

Measurement of glucose consumption, lactic acid production, and ATP production

Growth medium and cell filtrates were obtained to evaluate glucose intake and lactate production in 5-8F and CNE2 cells grown in 96-well plates. Glucose uptake levels were measured using a glucose uptake kit (BioVision, USA). Lactic acid was detected by lactic acid Kit II (BioVision), and ATP production was determined using ATP colorimetry (BioVision).

Reactive oxygen species (ROS) detection

5-8F and CNE2 cells (about 6×10^5 cells/wells) were inoculated into 6-well plates, collected by centrifugation, suspended in PBS, and loaded with 20 μ M dichloro-dihydro-fluorescein diacetate (DCFH-DA) at 37°C for 30 min. After that, cells were washed twice with PBS and analyzed immediately on a flow cytometer (Beckman Coulter) at 480 nm.

MMP assessment

MMP was assessed using the JC-1 test kit. 5-8F and CNE2 cells (5×10^5 cells/well) were inoculated on a 6-well plate, centrifuged, suspended in PBS, and stained with JC-1 at 37°C for 20 min. The cells were then collected and rinsed twice in JC-1 staining buffer (1 \times) and analyzed immediately using flow cytometry.

Oxidative stress index detection

Malondialdehyde (MDA), superoxide (SOD), and glutathione peroxidase (GSH-Px) in the cells were measured

using commercial kits (Nanjing Jiancheng Bioengineering Institute, Nanjing, China).

Western blot

Proteins were isolated from cells using radioimmunoprecipitation assay lysis buffer (Thermo Fisher) and quantified using a bicinchoninic acid kit (BioVision, USA). The proteins were separated on a 10% sodium dodecyl sulfate polyacrylamide gel and transferred to a polyvinylidene fluoride membrane (Thermo Fisher). The membrane was incubated in 5% milk and then with the primary antibody overnight and with the secondary antibody conjugated with horseradish peroxidase (BD Biosciences) at room temperature for 1 h. Protein bands were evaluated using the SynGene system and GeneSnap software (SynGene, USA). Primary antibodies: glyceraldehyde-3-phosphate dehydrogenase (2118, Cell Signaling Technology), cleaved caspase-3 (9664, Cell Signaling Technology), cleaved caspase-9, and cytochrome c (Cyto C) (37BA11, Invitrogen).

Data analysis

Data were expressed as mean \pm standard deviation (SD). All data were performed with at least five biological replicates. Normality test was conducted using Shapiro-Wilk, and bilateral comparison was compared by Student *t*-test whilst multiple comparisons were by one-way analysis of variance and Tukey HSD. $p < 0.05$ suggested a significant difference.

Results

Sev inhibits the malignant behaviors of NPC cells

To elucidate the effects of Sev on the biological characteristics of NPC cells, 5-8F and CNE2 cells were exposed to Sev at concentrations of 1.7%, 3.4%, and 5.1%. The results from the CCK-8 assay indicated a concentration-dependent suppression of cell proliferation upon Sev administration (Fig. 1A). Furthermore, colony formation assay demonstrated that treatment with Sev significantly curtailed the quantity of cellular colonies (Fig. 1B). We further examined the invasive and migratory capacities of these cells using Transwell assays. The data, as depicted in Figure 1C, show that Sev diminished the number of cells capable of invasion and migration in a concentration-dependent manner. Flow cytometric analysis post-Sev treatment revealed a notable elevation in cell apoptosis rates (Fig. 1D). These findings collectively underscore the potential of Sev in substantially impeding the malignant progression of NPC.

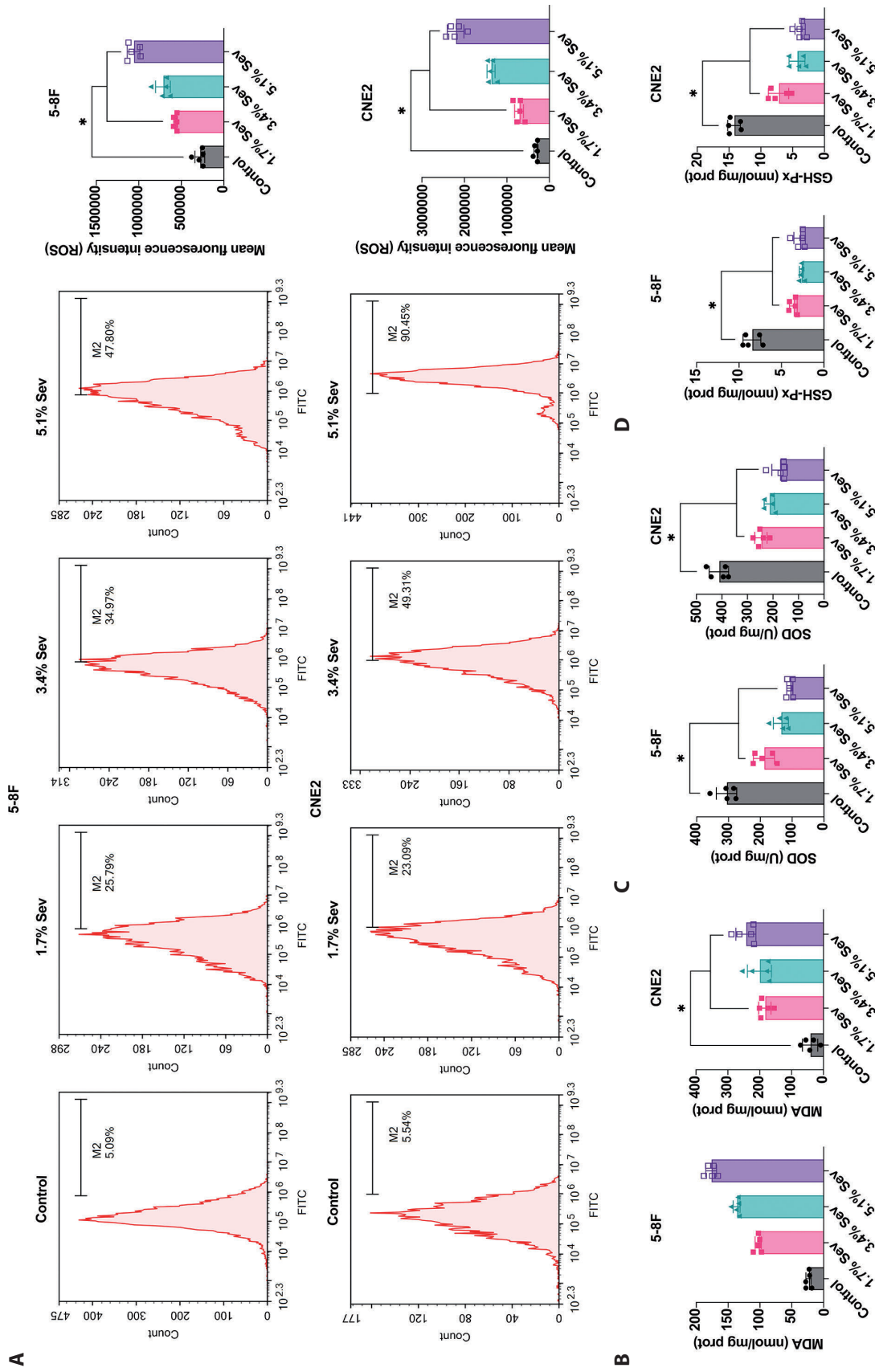


Figure 3. Sev effectively promoted ROS production in NPC. **A.** Fluorescence probe DCFH-DA and flow cytometry detected ROS changes in cells. Commercial kits detected MDA (**B**), SOD (**C**) and GSH-PX (**D**). Data were expressed as mean \pm SD ($n = 5$). * $p < 0.05$. For abbreviations, see Figure 1.

Sev effectively reduces the Warburg effect in NPC

Subsequently, we examined the impact of Sev on the Warburg effect in 5-8F and CNE2 cells. Demonstrated in Figure 2A, Sev significantly reduced glucose consumption at various concentrations. Moreover, lactate production, a hallmark of altered cancer metabolism, was also concentration-dependently decreased by Sev, as shown in Figure 2B. Notably, Sev treatment led to a reduction in ATP production, evident in Figure 2C. We further investigated the expression of Warburg effect-related proteins through Western blot. Figure 2D shows that Sev notably decreased the expression of hexokinase 2 (HK2) and pyruvate kinases type M2 (PKM2), key enzymes in glycolytic pathways. These findings collectively underscore that Sev exerts a dose-dependent suppression of the Warburg effect in NPC cells, shedding light on its potential role in modulating cancer cell metabolism.

Sev effectively promotes ROS production in NPC

To probe the linkage between Sev-induced apoptosis and the suppression of proliferation, invasion, and migration in NPC cells with ROS generation, we assessed intracellular ROS dynamics *via* the DCFH-DA fluorescent probe. Figure 3A illustrates a dose-dependent escalation in ROS concentrations upon Sev administration. Furthermore, subsequent to Sev exposure, an upsurge in MDA levels was observed, concurrent with a decline in SOD and GSH-PX concentrations (Fig. 3B–D). These outcomes suggest that Sev significantly enhances ROS production, thereby precipitating cellular oxidative damage – a pivotal insight into its mechanistic role in cancer cell modulation.

Sev effectively disrupts mitochondrial homeostasis in NPC cells

Mitochondrial dysfunction, marked by reduced membrane potential, is a key precursor to ROS generation. In this context, we probed the effect of Sev on the MMP of 5-8F and CNE2 cells. Employing the JC-1 probe for assessing MMP alterations, our findings, as presented in Figure 4A, revealed that Sev induced a concentration-dependent decrease in MMP. Subsequent analysis focused on mitochondrial apoptotic pathway proteins. Figure 4B shows a significant upregulation in the levels of cleaved caspase-3, cleaved caspase-9, and Cyto C post-Sev treatment. These results underscore Sev's capacity to dose-dependently destabilize mitochondrial equilibrium, lowering MMP in NPC cells, and thus triggering apoptosis.

Discussion

NPC is a malignant head and neck tumor with a high incidence in Southeast Asia, but its pathogenesis remains

unclear. Sev is a kind of anesthetic widely used in surgery and is considered a safe reagent for clinical use (Yu and Bai 2022). In the context of NPC, this paper probed the specific mechanism of Sev in controlling tumor cell malignant progression. As discovered, Sev prevented NPC cells from malignant growth by MMP regulation.

Sev has the opposite effect on cancer progression, depending on its concentration and the type of cancer (Hirai et al. 2020; Yun et al. 2023). Given that, this research on NPC studied the action of Sev at different concentrations (1.7%, 3.4%, and 5.1%). As the results observed, Sev affected NPC cell activities in a concentration-dependent way. To start, Sev treatment suppressed NPC cell proliferation by decreasing cellular proliferative rate and the number of cell clones. The inhibition of mitochondrial function leads to the disturbance of cell energy metabolism and affects the regulation of key points of cell cycle (Luo et al. 2020). Cells may not successfully pass the G1/S or G2/M checkpoint, resulting in cell cycle arrest (Leal-Esteban and Fajas 2020). Such changes directly affect the cell's ability to proliferate and reduce the number of cell clones, as observed in the study. Also, Sev treatment dampened NPC cell invasion and migration, whilst elevating cell apoptosis rate. Due to the central role of mitochondria in regulating apoptosis, inhibition of mitochondrial function leads to activation of apoptosis signaling pathways. Increased permeability of the mitochondrial outer membrane leads to the release of apoptosis-effector molecules such as Cyto C, activation of caspase family proteins, and ultimately an increase in apoptosis (Bock and Tait 2020). In accordance with a published paper, Sev exerts a time-dependent and dose-dependent effect on the proliferation/migration inhibition rate of gastric cancer cells (Chen et al. 2020). Additionally, Sev shows concentration-dependent migration and invasion inhibition of colorectal cancer cells, in which the mechanism is mediated by the extracellular signal-regulated kinase/matrix metalloproteinase-9 pathway and miR-203/Robo1 axis (Fan et al. 2019). The fact that Sev represses ovarian cancer cell proliferation, migration, and invasion and induces apoptosis, and these effects are positively correlated with Sev dose have been determined (Kang and Wang 2019). Remarkably, Sev has been reported to reduce viability and even stimulate apoptosis of laryngeal squamous cell carcinoma cells by upregulating miR-26a-targeted Forkhead Box Protein O1 (Liu et al. 2021). Meanwhile, Yang et al. (2018) have checked the significant inhibition of head and neck squamous cell carcinoma cell growth following Sev exposure at different concentrations (2 and 4%). In combination with these reports, our study further supported the anti-tumor potential of Sev.

Tumor cells maintain and induce long-term survival by trimming metabolism, which is characterized by increased glucose uptake and the fermentation of glucose into lactic

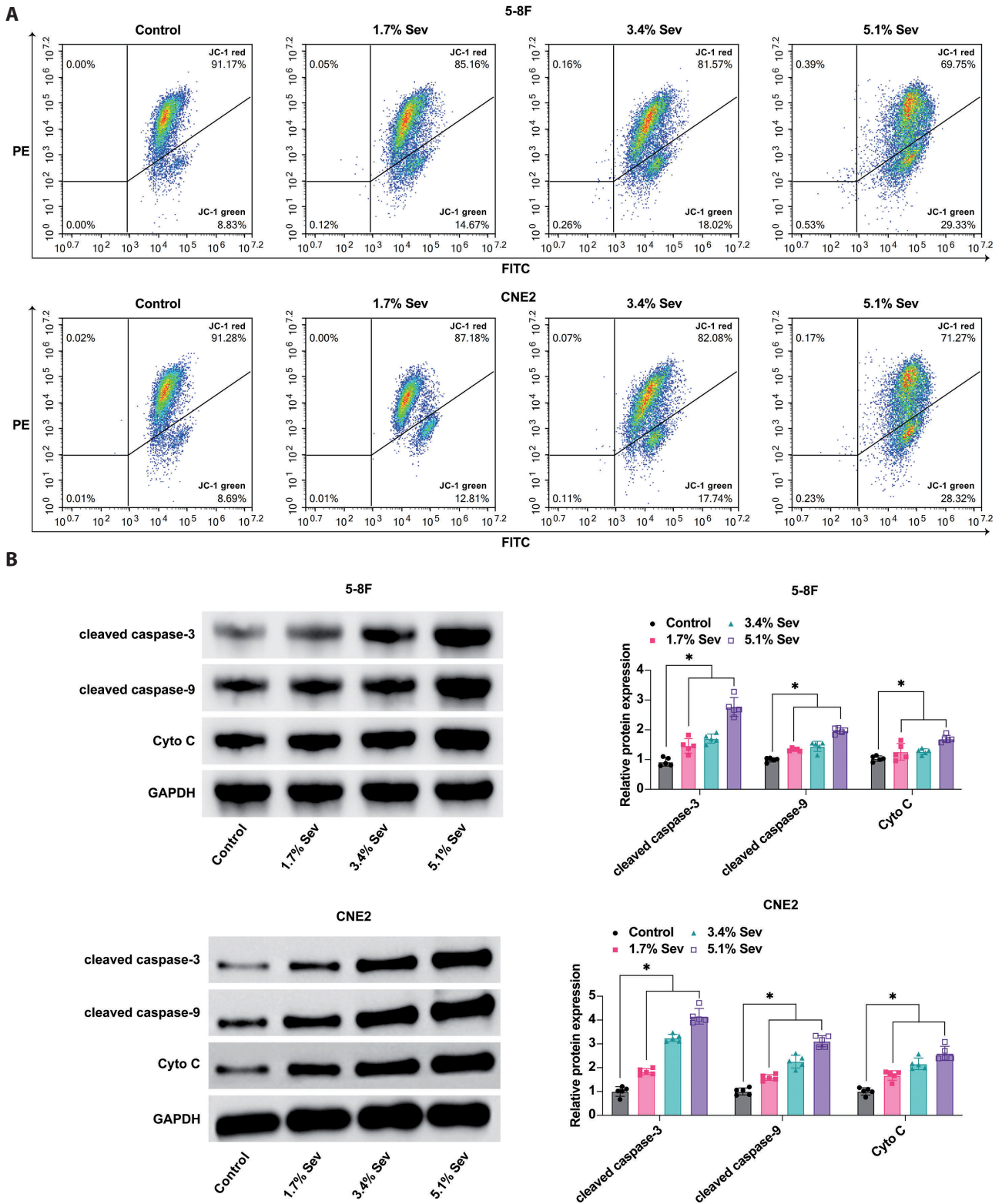


Figure 4. SeV effectively disrupts mitochondrial homeostasis in NPC cells. **A.** The changes of mitochondrial membrane potential (MMP) were detected by JC-1 probe and flow cytometry. **B.** Mitochondrial apoptosis pathway-related proteins, cleaved caspase-3, cleaved caspase-9, and cytochrome c (Cyto C), were detected by Western blot. Data were expressed as mean \pm SD ($n = 5$). * $p < 0.05$. For abbreviations, see Figure 1.

acid. This phenomenon is observed even when mitochondria function is perfectly normal and is known as the “Warburg effect” (Liberti and Locasale 2016). In this work, it could be observed that Sev suppressed glucose consumption, lactate production, ATP production, and protein expression of HK2 and PKM2 to achieve an anti-glycolytic effect on NPC cells. However, if mitochondrial function is impaired, tumor cells may not be able to effectively use oxidative phosphorylation to produce energy, leading to energy crisis and metabolic stress (Wu et al. 2022). Consistently, a study has obtained validation of the effective role of Sev to prevent glycolysis and proliferation in lung cancer (Sun et al. 2022). ROS can activate pro-tumor signaling, enhance cell survival and proliferation, and drive DNA damage and genetic instability. Besides, ROS also initiates oxidative stress-induced tumor cell death, and tumor cells express high levels of antioxidant proteins to detoxify elevated ROS levels and establish a REDOX balance while maintaining pro-tumor signaling and resistance to apoptosis (Moloney and Cotter 2018). Here, our study noticed that Sev increased ROS production and oxidative injury in NPC cells, as well as damaged mitochondrial homeostasis by upregulating cleaved caspase-3, cleaved caspase-9, and Cyto C protein expressions. Notably, Sev can suppress the mitochondrial function of glioma cells by promoting ROS production and reducing MMP (Han et al. 2020). At present, the downside is that not enough evidence can further prove the action of Sev in mitochondrial dysfunction and oxidative injury in the tumor microenvironment.

Collectively, this research confirms the anti-NPC action of Sev through suppression of tumor growth and disruption of mitochondrial homeostasis. The main conclusion has provided more possibilities for Sev application in tumor treatment. Nevertheless, the molecules and signaling pathways involved in Sev-mediated management of NPC development are not identified in the current study.

Conflict of interest. The authors have no conflicts of interest to declare.

Data available. Data is available from the corresponding author on request.

Authors’ contributions. XP designed the research study. XP and YZ performed the research. YZ provided help and advice on the experiments. XP and YZ analyzed the data. XP wrote the manuscript. YZ reviewed and edited the manuscript. All authors contributed to editorial changes in the manuscript. All authors read and approved the final manuscript.

References

- Barreiro E, Bustamante V, Curull V, Gea J, Lopez-Campos JL, Munoz X (2016): Relationships between chronic obstructive pulmonary disease and lung cancer: biological insights. *J. Thor. Dis.* **8**, E1122-E1135
<https://doi.org/10.21037/jtd.2016.09.54>
- Booton R, Lindsay MA (2014): Emerging role of MicroRNAs and long noncoding RNAs in respiratory disease. *Chest* **146**, 193-204
<https://doi.org/10.1378/chest.13-2736>
- Bray F, Ferlay J, Soerjomataram I, Siegel RL, Torre LA, Jemal A (2018): Global cancer statistics 2018: GLOBOCAN estimates of incidence and mortality worldwide for 36 cancers in 185 countries. *CA Cancer J. Clin.* **68**, 394-424
<https://doi.org/10.3322/caac.21492>
- Chen LL (2016): The biogenesis and emerging roles of circular RNAs. *Nat. Rev. Mol. Cell. Biol.* **17**, 205-211
<https://doi.org/10.1038/nrm.2015.32>
- Chen T, Yang Z, Liu C, Wang L, Yang J, Chen L, Li W (2019): Circ_0078767 suppresses non-small-cell lung cancer by protecting RASSF1A expression via sponging miR-330-3p. *Cell. Prolif.* **52**, e12548
<https://doi.org/10.1111/cpr.12548>
- Chen X, Yuan Q, Liu J, Xia S, Shi X, Su Y, Wang Z, Li S, Shang D (2022): Comprehensive characterization of extracellular matrix-related genes in PAAD identified a novel prognostic panel related to clinical outcomes and immune microenvironment: A silico analysis with in vivo and vitro validation. *Front. Immunol.* **13**, 985911
<https://doi.org/10.3389/fimmu.2022.985911>
- Henrot P, Prevel R, Berger P, Dupin I (2019): Chemokines in COPD: from implication to therapeutic use. *Int. J. Mol. Sci.* **20**, 2785
<https://doi.org/10.3390/ijms20112785>
- Jin M, Shi C, Yang C, Liu J, Huang G (2019): Upregulated circRNA ARHGAP10 predicts an unfavorable prognosis in NSCLC through regulation of the miR-150-5p/GLUT-1 axis. *Mol. Ther. Nucleic Acids* **18**, 219-231
<https://doi.org/10.1016/j.omtn.2019.08.016>
- Kneidinger N, Yildirim AO, Callegari J, Takenaka S, Stein MM, Dumitrascu R, Bohla A, Bracke KR, Morty RE, Brusselle GG, et al. (2011): Activation of the WNT/beta-catenin pathway attenuates experimental emphysema. *Am. J. Resp. Crit. Care Med.* **183**, 723-733
<https://doi.org/10.1164/rccm.200910-1560OC>
- Li R, Qu H, Wang S, Chater JM, Wang X, Cui Y, Yu L, Zhou R, Jia Q, Traband R, et al. (2022): CancerMIRNome: an interactive analysis and visualization database for miRNome profiles of human cancer. *Nucleic Acids Res.* **50**, D1139-D1146
<https://doi.org/10.1093/nar/gkab784>
- Li S, Teng S, Xu J, Su G, Zhang Y, Zhao J, Zhang S, Wang H, Qin W, Lu ZJ, et al. (2019): Microarray is an efficient tool for circRNA profiling. *Brief. Bioinform.* **20**, 1420-1433
<https://doi.org/10.1093/bib/bby006>
- Licker MJ, Widikker I, Robert J, Frey JG, Spiliopoulos A, Tschopp JM (2006): Operative mortality and respiratory complications after lung resection for cancer: impact of chronic obstructive pulmonary disease and time trends. *Ann. Thorac. Surg.* **81**, 1830-1837
<https://doi.org/10.1016/j.athoracsur.2005.11.048>
- Ma Q, Li L, Yu B, Jiao L, Han Z, Zhao H, Li G, Ma Y, Luo Y (2019): Circular RNA profiling of neutrophil transcriptome provides insights into asymptomatic Moyamoya disease. *Brain Res.* **1719**, 104-112

- <https://doi.org/10.1016/j.brainres.2019.05.033>
- Ma Y, Yuan Q, He S, Mao X, Zheng S, Chen C (2022): Characterizing the prognostic and therapeutic value of necroptosis in sarcoma based on necroptosis subtypes. *Front. Genet.* **13**, 980209 <https://doi.org/10.3389/fgene.2022.980209>
- Mei D, Tan WSD, Tay Y, Mukhopadhyay A, Wong WSF (2020): Therapeutic RNA strategies for chronic obstructive pulmonary disease. *Trends Pharmacol. Sci.* **41**, 475-486 <https://doi.org/10.1016/j.tips.2020.04.007>
- Mestdagh P, Vandesompele J, Brusselle G, Vermaelen K (2015): Non-coding RNAs and respiratory disease. *Thorax* **70**, 388-390 <https://doi.org/10.1136/thoraxjnl-2014-206404>
- Nicot C (2019): RNA-Seq reveal the circular RNAs landscape of lung cancer. *Mol. Cancer* **18**, 183 <https://doi.org/10.1186/s12943-019-1118-8>
- Norman KC, Freeman CM, Bidthanapally NS, Han MK, Martinez FJ, Curtis JL, Arnold KB (2019): Inference of cellular immune environments in sputum and peripheral blood associated with acute exacerbations of COPD. *Cell. Mol. Bioeng.* **12**, 165-177 <https://doi.org/10.1007/s12195-019-00567-2>
- Parris BA, O'Farrell HE, Fong KM, Yang IA (2019): Chronic obstructive pulmonary disease (COPD) and lung cancer: common pathways for pathogenesis. *J. Thorac. Dis.* **11**, S2155-S2172 <https://doi.org/10.21037/jtd.2019.10.54>
- Reck M, Rabe KF (2017): Precision diagnosis and treatment for advanced non-small-cell lung cancer. *New Engl. J. Med.* **377**, 849-861 <https://doi.org/10.1056/NEJMra1703413>
- Ruano-Ravina A, Mouronte-Roibás C, Fernández-Villar A, Fernández V, Ramos-Hernández C, Botana-Rial M (2016): COPD, emphysema and the onset of lung cancer. A systematic review. *Cancer Letters* **382**, 240-244 <https://doi.org/10.1016/j.canlet.2016.09.002>
- Singh D, Agusti A, Anzueto A, Barnes PJ, Bourbeau J, Celli BR, Criner GJ, Frith P, Halpin DMG, Han M, et al. (2019): Global strategy for the diagnosis, management, and prevention of chronic obstructive lung disease: the GOLD science committee report 2019. *Eur. Resp. J.* **53**, 1900164 <https://doi.org/10.1183/13993003.00164-2019>
- Skillrud DM, Offord KP, Miller RD (1986): Higher risk of lung cancer in chronic obstructive pulmonary disease. A prospective, matched, controlled study. *Ann. Int. Med.* **105**, 503-507 <https://doi.org/10.7326/0003-4819-105-4-503>
- Szabo L, Salzman J (2016): Detecting circular RNAs: bioinformatic and experimental challenges. *Nat. Rev. Gen.* **17**, 679-692 <https://doi.org/10.1038/nrg.2016.114>
- Trivedi A, Khan MA, Bade G, Talwar A (2021): Orchestration of neutrophil extracellular traps (Nets), a unique innate immune function during chronic obstructive pulmonary disease (COPD) development. *Biomedicines* **9**, 53 <https://doi.org/10.3390/biomedicines9010053>
- Vo JN, Cieslik M, Zhang Y, Shukla S, Xiao L, Zhang Y, Wu YM, Dhanasekaran SM, Engelke CG, Cao X, et al. (2019): The landscape of circular RNA in cancer. *Cell* **176**, 869-881.e13 <https://doi.org/10.1016/j.cell.2018.12.021>
- Vogelmeier CF, Criner GJ, Martinez FJ, Anzueto A, Barnes PJ, Bourbeau J, Celli BR, Chen R, Decramer M, Fabbri LM, et al. (2017): Global strategy for the diagnosis, management, and prevention of chronic obstructive lung disease 2017 report. GOLD executive summary. *Am. J. Resp. Crit. Care Med.* **195**, 557-582 <https://doi.org/10.1164/rccm.201701-0218PP>
- Vos T, Abajobir AA, Abate KH, Abbafati C, Abbas KM, Abd-Allah F, Abdulkader RS, Abdulle AM, Abebo TA, Abera SF, et al. (2017): Global, regional, and national incidence, prevalence, and years lived with disability for 328 diseases and injuries for 195 countries, 1990-2016: a systematic analysis for the Global Burden of Disease Study 2016. *Lancet* **390**, 1211-1259 [https://doi.org/10.1016/S0140-6736\(17\)32154-2](https://doi.org/10.1016/S0140-6736(17)32154-2)
- Vyse S, Huang PH (2019): Targeting EGFR exon 20 insertion mutations in non-small cell lung cancer. *Signal. Transduct. Target Ther.* **4**, 5 <https://doi.org/10.1038/s41392-019-0038-9>
- Wang H, Yang D, Xu W, Wang Y, Ruan Z, Zhao T, Han J, Wu Y (2008): Tumor-derived soluble MICs impair CD3(+)CD56(+) NKT-like cell cytotoxicity in cancer patients. *Immunol. Lett.* **120**, 65-71 <https://doi.org/10.1016/j.imlet.2008.07.001>
- Wilson DO, Weissfeld JL, Balkan A, Schragin JG, Fuhrman CR, Fisher SN, Wilson J, Leader JK, Siegfried JM, Shapiro SD, et al. (2008): Association of radiographic emphysema and airflow obstruction with lung cancer. *Am. J. Resp. Crit. Care Med.* **178**, 738-744 <https://doi.org/10.1164/rccm.200803-435OC>
- Xia P, Wang S, Ye B, Du Y, Li C, Xiong Z, Qu Y, Fan Z (2018): A circular RNA protects dormant hematopoietic stem cells from DNA sensor cGAS-mediated exhaustion. *Immunity* **48**, 688-701.e7 <https://doi.org/10.1016/j.immuni.2018.03.016>
- Yuan Q, Zhang W, Shang W (2022): Identification and validation of a prognostic risk-scoring model based on sphingolipid metabolism-associated cluster in colon adenocarcinoma. *Front. Endocrinol.* **13**, 1045167 <https://doi.org/10.3389/fendo.2022.1045167>
- Zeng N, Wang T, Chen M, Yuan Z, Qin J, Wu Y, Gao L, Shen Y, Chen L, Wen F (2019): Cigarette smoke extract alters genome-wide profiles of circular RNAs and mRNAs in primary human small airway epithelial cells. *J. Cell. Mol. Med.* **23**, 5532-5541 <https://doi.org/10.1111/jcmm.14436>
- Zhao M, Gao F, Zhang D, Wang S, Zhang Y, Wang R, Zhao J (2017): Altered expression of circular RNAs in Moyamoya disease. *J. Neurol. Sci.* **381**, 25-31 <https://doi.org/10.1016/j.jns.2017.08.011>
- Zhou Y, Zheng X, Xu B, Chen L, Wang Q, Deng H, Jiang J (2019): Circular RNA hsa_circ_0004015 regulates the proliferation, invasion, and TKI drug resistance of non-small cell lung cancer by miR-1183/PDPK1 signaling pathway. *Biochem. Biophys. Res. Commun.* **508**, 527-535 <https://doi.org/10.1016/j.bbrc.2018.11.157>
- Zhu D, Yu Y, Wang W, Wu K, Liu D, Yang Y, Zhang C, Qi Y, Zhao S (2019): Long noncoding RNA PART1 promotes progression of non-small cell lung cancer cells via JAK-STAT signaling pathway. *Cancer Med.* **8**, 6064-6081 <https://doi.org/10.1002/cam4.2494>

Received: October 24, 2023

Final version accepted: March 12, 2024